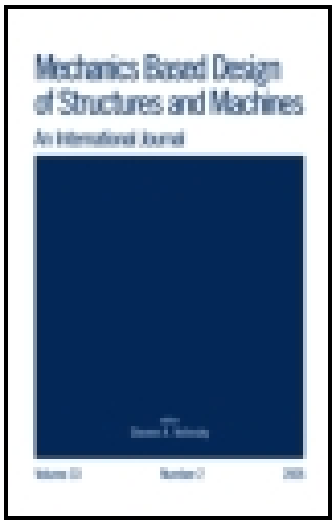

Mechanics Based Design of Structures and Machines: An International Journal

Publication details, including instructions for authors and subscription information:
http://www.tandfonline.com/loi/lmbd20

# Kinematics, Efficiency and Dynamic Balancing of a Planetary Gear Train Based on Nutating Bevel Gears

P. Fanghella[a], L. Bruzzone[a], S. Ellero[b] & R. Landò[b]

[a] University of Genoa, Italy

[b] Stam Srl, Genoa, Italy

Accepted author version posted online: 14 Jun 2015.

# Kinematics, Efficiency and Dynamic Balancing of a Planetary Gear Train Based on Nutating Bevel Gears

P. Fanghella[1], L. Bruzzone[1], S. Ellero[2], R. Landò[2]

[1]University of Genoa, Italy [2]Stam Srl, Genoa, Italy

Corresponding author P. Fanghella University of Genoa, Italy E-mail: pietro.fanghella@unige.it





## Abstract

The paper discusses the main functional characteristics of a planetary gear train based on nutating bevel gears. System geometry, design parameters, kinematics and efficiency expressions in term of such parameters are presented. Then an analytical model of its dynamics is developed and explicit balancing conditions to eliminate the effect of internal inertial forces are obtained. Analytical results regarding dynamics and balancing criteria are verified through multibody simulations on a sample geometry. A discussion about how to determine balancing geometries is finally carried out.

**KEYWORDS:** Planetary gear train, bevel gears, nutation, mechanism design, dynamic balancing.

## 1. INTRODUCTION

Planetary gear trains represent an important class of mechanical transmissions, used in a wide variety of applications. When very compact solutions and high transmission ratios are required, special configurations based on bevel gears become interesting (Molyneux, 1997; Litvin and Zheng, 1986; Barbagelata et al., 2003). This particular type of planetary gear trains has been extensively studied from a kinematic point of view, see Molyneux

(1997), Litvin and Zheng (1986), Day et al. (1983), Nelson and Cipra (2005-a), Uyguroglu and Demirel (2005) and Talpasanu and Simionescu (2012), and in order to evaluate the efficiency and power-flows of different configurations, see for example Nelson and Cipra (2005-b), Del Pio et al. (2013) and Fanghella (2009). Only a limited number of results, especially for the bevel gear mechanisms, is available regarding mechanism dynamics: beyond specific results regarding gear meshing (Ligang et al., 2010), for example Staicu (2008) discusses the internal inverse dynamics (torques and forces) of a bevel gear train used in robotic applications. Moreover, some specific contributions are available regarding the type of mechanism considered in the present paper, i.e., a planetary gear train based on nutating bevel gears (Landò, 2001). In particular, beyond the cited contribution of Molyneux (1997), Ligang et al. (2010) consider the meshing of gears in this specific type of train, and Zihni et al. (2013) analyze its application, based on face gears, to a specific aeronautic problem.

Starting from a real geometric configuration, this paper considers all main functional characteristics of a nutating bevel gearbox. First, geometrical design parameters and their relations with input/output kinematics are analyzed. Then power flow and efficiency relations are presented, again in terms of geometrical and functional parameters. Although the considered geometry is not new (Molyneux, 1997; Ligang et al., 2010; Zihni et al., 2013) - the paper yields explicit relations among geometry design angles on one side and gearbox transmission ratio and efficiency on the other, not provided elsewhere.

In the second part of the paper, a peculiar aspect of the dynamics of planetary bevel gear trains is considered: due to their embodiment geometries and to the presence of bodies rotating around moving axes, this kind of mechanism, even in steady state conditions, are characterized by both unbalanced geometries for rotating bodies and angular velocities rapidly varying in direction. Accordingly, they possibly present centrifugal and gyroscopic effects that, at high speed, can transmit high inertial loads - forces and torques - to the system frame. This feature, typical of this type of gearboxes, is not usually considered in scientific literature, as the analysis and design processes usually terminate at the conceptual stage, except in very few cases, see for example Zihni et al. (2013). Therefore, it is relevant to assess the conditions required to have both static and dynamic balancing for this kind of gearboxes (Yan et al., 2005).

Concerning this aspect, the paper looks for the solution with regards to the mechanism discussed in the first part of the paper, developing explicit results for its geometry. In general, the presented approach can be applied to any other mechanism of this type: explicit balancing are obtained by a fully analytical model of the inverse dynamics of the gearbox, treated as an open chain, based on Newton-Euler equations.

Thr analytical results obtained in Section 5 are then validated by numerical multibody analyses in Section 6

Finally, actual application of the mathematical balancing conditions to the embodiment design of gearbox bodies is discussed in Section 7.

The presented approach to dynamic balancing discussed in Sections 4, 5 and 7, here applied to a specific type of nutating gearbox, is general and systematic and can be applied to any type of planetary gear train, based on bevel gears, also in presence of gyroscopic complexity, as those discussed in Del Pio et al. (2013). The inertial balancing of such gearbox types is critical in their real design, as, for high values of the input speed, common in small high performance actuators, the vibrations induced by those excitations, in case of unbalanced geometry, may significantly hinder their feasibility for engineering applications.

## 2. GEOMETRY AND INPUT-OUTPUT KINEMATICS

Figure 1 presents a scheme of the mechanism:

- the mechanism frame is body 1; a gear wheel ($z_{1\_g1}$) is attached to it
- the input shaft, body 2, constituting the gear train carrier, is connected to the frame by the revolute joint $R_{12}$, and to the nutating gear (body 3) by the revolute joint $R_{23}$
- the output shaft and the gear wheel attached to it ($z_{4\_g2}$) constitute body 4, which is connected to the frame by the revolute joint $R_{14}$, coaxial with $R_{12}$
- the nutating body 3 is attached by the revolute joint $R_{23}$ to the carrier and by the two gears $g_1$ and $g_2$ to the frame and the output shaft respectively. The axis of $R_{23}$ intersects the common axis of $R_{12}$ and $R_{14}$ at point **O**, that is the center of the spherical motion of all bodies; the angle □ between the joint axes is fixed by the shape of the carrier body and constitutes one of the key parameters of the mechanism.

Figure 1 also shows the two bevel gearings in the planetary gear train:

- $g_1$ connecting bodies 3 and 4 (traces of primitive cones in white)
- $g_2$ connecting bodies 3 and 1 (traces of primitive cones in grey)

Let us consider a O,x,y,z reference frame (Figure 2), with x-y plane containing the axes of all three revolute pairs. Beyond angle $\alpha$, two further design parameters may be introduced:

- the angle $\beta$ from the x-axis to the pitch cone of gear $g_1$ (negative in Figure 2)

the angle $\delta$ from the x-axis to the pitch cone of gear $g_2$ (positive in Figure 2)

The four angles of the pitch cones (Figure 2) can be expressed as functions of the three design angles:

$$\alpha_{13} = \frac{\pi}{2} - \beta \qquad (1)$$

$$\alpha_{31} = \frac{\pi}{2} - \alpha + \beta \qquad (2)$$

$$\alpha_{43} = \frac{\pi}{2} - \delta \qquad (3)$$

$$\alpha_{34} = \frac{\pi}{2} - \alpha + \delta \qquad (4)$$

The mechanism has two independent loops (1-$R_{12}$-2-$R_{23}$-3-$g_1$-1) and (1-$R_{12}$-2-$R_{23}$-3-$g_2$-4-C-1). The analysis of the first one can be carried out and solved without taking into account of the second, so, given the velocity of the input link 2 ($\omega_{12}=\omega_{12y}$) with respect to fixed link 1, the ratios of the relative velocity between link 3 and link 2 ($\omega_{23}$), and of the

angular velocity of link 3 w.r.t. link 1, $\omega_{13}$, with input velocity $\omega_{12}$, can be determined according to the following congruence equations, in which $\omega_{13y}$, $\omega_{13x}$ represent the axial and radial components of $\omega_{13}$:

$$\begin{cases} \omega_{13x} = \omega_{23x} & \omega_{12x} = 0 \\ \omega_{13y} = \omega_{12y} + \omega_{23y} & \omega_{12y} = \omega_{12} \\ \omega_{13x} = \omega_{13}\cos\ \beta \\ \omega_{13y} = \omega_{13}\sin\ \beta \\ \omega_{23x} = \omega_{23}\cos\ \alpha - \pi/2 \\ \omega_{23y} = \omega_{23}\sin\ \alpha - \pi/2 \end{cases} \tag{5}$$

Then by solving, the following relations are obtained:

$$\frac{\omega_{13x}}{\omega_{12}} = \frac{\sin\ \alpha\ \cos\ \beta}{\cos\ \alpha - \beta};\quad \frac{\omega_{13y}}{\omega_{12}} = \frac{\sin\ \alpha\ \sin\ \beta}{\cos\ \alpha - \beta} \tag{6}$$

$$\tau_{32\_2} = \frac{\omega_{23}}{\omega_{12}} = \frac{\cos\ \beta}{\cos\ \alpha - \beta} \tag{7}$$

$$\tau_{32} = \frac{\omega_{13}}{\omega_{12}} = \frac{\sin\ \alpha}{\cos\ \alpha - \beta} \tag{8}$$

Then the second loop can similarly be solved, starting from link 3, finally obtaining the ratio between the input and output ($\omega_{14}$=$\omega_{14y}$) velocities, i.e., the reduction ratio $\tau_{42}$ of the gearbox:

$$\tau_{42} = \frac{\omega_{14}}{\omega_{12}} = \frac{\sin\ \alpha\ \sin\ \beta - \delta}{\cos\ \delta\ \cos\ \alpha - \beta} \tag{9}$$

By substitution, the same velocity ratio can be expressed as a function of the bevel gear pitch angles and of their tooth numbers:

$$\tau_{42} = \frac{\omega_{14}}{\omega_{12}} = 1 - \frac{\sin\ \alpha_{13}\ \sin\ \alpha_{34}}{\sin\ \alpha_{31}\ \sin\ \alpha_{43}} = 1 - \frac{z_{1\_g1} z_{3\_g2}}{z_{3\_g1} z_{4\_g2}} = 1 - \tau_{g1c}\tau_{g2c} \tag{10}$$

A further geometrical arrangement is possible for the same topology. In this case, angles $\alpha$, $\beta$ and $\delta$ must be measured as shown in Figure 3 (all positive in the figure). With this angle convention all previous relations hold also for this second configuration.

The main difference between the two configurations is the geometry of the nutating link 3. In the first configuration (Figure 2), the teeth of the two gears on such link lay on the same side and, therefore, they must be inserted one inside the other in some way, as shown in the 3D geometry in Figure 4-a). In the second configuration (Figure 3), the gears are on the opposite sides of the planet, so the two gears may have similar tooth dimensions for similar numbers of tooth, as shown in in Figure 4-b). This variation affects significantly the architecture of the speed reducer in term of compactness, capacity of load carrying, bearing location, static and dynamic balancing.

The previous relations provide hints about mechanism design. First of all, the output velocity vanishes when: 1) the angle $\alpha$ is null; 2) the angles $\beta$ and $\delta$ are equal. Accordingly, very high transmission ratios can be obtained by approaching such limit conditions. Then, for positive values of angle $\alpha$ $\tau_{42}$ is positive if $\beta - \delta > 0$. Moreover, the gear train is a speed reducer if $-1 < \tau_{42} < 1$. For a design procedure, given the desired transmission ratio $\tau_{42}$, a tentative value of the angle $\alpha$ can be chosen; then, by selecting proper values for the velocity ratios of the two bevel gears $g_1$ and $g_2$ ($\tau_{g1c}$ and $\tau_{g2c}$), compatible with equation (10), the angles $\beta$ and $\delta$ can be obtained by the following relations:

$$\delta = \arctan\left(\frac{\tau_{g2c} - \cos\ \alpha}{\sin\ \alpha}\right) \qquad (11)$$

$$\beta = -\arctan\left(\frac{\tau_{g1c}\cos\ \alpha\ -1}{\tau_{g1c}\sin\ \alpha}\right) \qquad (12)$$

Then the pitch angles $\alpha_{ij}$ for the two gear pairs can be readily computed by equations 1-4, and checks for the feasibility of tooth numbers, modules and geometry can be carried out.

## 3. GEAR TRAIN POWER FLOW AND EFFICIENCY

Similarly to most results available in scientific literature (see Nelson and Cipra, (2005-a); Del Pio et al., (2013); Fanghella (2009)), the evaluation of the reducer efficiency will be carried out by taking into account only of the losses in the gears, and by neglecting other losses of minor importance, such as those in bearings.

In order to assess the efficiency of the considered solution and to express it in terms of the geometric design parameters, a generic bevel gear pair is first considered (Figure 5). The input and output gears are connected to the carrier link by pairs $R_i$ and $R_o$, and in direct contact through the gear pair g. Relative velocities between the carrier and the two gears are respectively $\omega_{rel\_i}$ and $\omega_{rel\_o}$.

Instead of considering the loop equilibrium and power balance equations, which are of impractical use due to the non-planar geometry of planetary trains based on bevel gears, the concept of power flowing through the gear g is introduced (Figure 6), and expressed through the following relation:

$$PF_i - PF_o - P_l = \omega_{rel\_i} T_i - \omega_{rel\_o} T_o - P_l = 0 \quad (13)$$

in which $T_i$ and $T_o$ are respectively the input and output torques of gear *g* and $P_l$ is the lost power.

If gear *g* has an efficiency $\eta_g$, the previous relation becomes:

$$\eta_g PF_i - PF_o = \eta_g \omega_{rel\_i} T_i - \omega_{rel\_o} T_o = 0 \qquad (14)$$

and the power lost in gear g is:

$$P_l = (1-\eta_g)\, PF_i = (1-\eta_g)\, \omega_{rel\_i} T_i \qquad (15)$$

By applying Eqs. 14 and 15 and the kinematic relations developed in the previous Section to the two gears of the complete gear train, it is possible to obtain the expression of its efficiency as a function of the design parameters and of the elementary efficiencies of the two gears $g_1$ and $g_2$.

Let us consider a general case and assume, to obtain normalized relations, that input velocity $\omega_2$ and output torque $T_4$ are known. In the ideal case, for which $\eta_{g1} = \eta_{g2} = 1$, the input and output powers are

$$P_{i\_id} = P_o = \omega_{12} T_{12} = \omega_{14} T_{14} = \tau_{42} \omega_{12} T_{14} \qquad (16)$$

and the input torque is

$$T_{12} = \tau_{42} T_{14} \qquad (17)$$

In the real case, the power balance must be applied twice, for the two gears:

- GEAR $g_2$: to apply Eq. 14, known terms must be made explicit:

- $T_{o\_g2} = T_{14}$
- $\omega_{rel\_i\_g2} = \omega_{23}$
- $\omega_{rel\_i\_g2} = \omega_{14} - \omega_{12}$

Then, the input torque for gear $g_2$ is obtained from Eq. 14:

$$T_{i\_g2} = \pm \frac{T_{14} \cos\ \alpha - \delta}{\eta_{g2} \cos\ \delta} \qquad (18)$$

in which, due to the different sign of the input power flow, the + and - signs apply respectively to negative and positive values of the transmission ratio $\tau_{42}$.

- GEAR $g_1$: the input torque of $g_2$ is the output torque to $g_1$, for which input and output links are respectively planet 3 and sun 1. Then, for $g_2$, Eq. 14 becomes:

- $T_{o\_g1} = T_{i\_g2}$
- $\omega_{rel\_i\_g1} = \omega_1 - \omega_{12} = -\omega_{12}$ since $\omega_1 = 0$
- $\omega_{rel\_u\_g2} = \omega_{23}$

$$T_{i\_g1} = \frac{T_{i\_g2}\omega_{32}}{\eta_{g1}\omega_{12}} = \mp \frac{T_{14} \cos\ \alpha - \delta\ \cos\ \beta}{\eta_{g1}\eta_{g2} \cos\ \alpha - \beta\ \cos\ \delta} \qquad (19)$$

For both gears, equations for power flows and power losses may be directly obtained from Eqs. 14 and 15. Then the efficiency of the reducer may be obtained as the ratio of the output and real input powers (all assumed positive):

$$\eta = \frac{P_o}{P_o + P_{l\_g1} + P_{l\_g2}} \qquad (20)$$

By substitution of all quantities, an explicit expressions of such efficiency in term of the design parameters of the reducer may be obtained. The power flows for positive and negative values of the transmission ratio $\tau_{42}$ differ, due to different signs in output angular velocities. So two distinct expression are obtained:

- Positive $\tau_{42}$

$$\eta_{\tau+} = \frac{\eta_{g1}\eta_{g2} \sin\ \alpha\ \sin\ \beta - \delta}{\eta_{g1}\eta_{g2}\ \sin\ \alpha\ \sin\ \beta - \delta\ - \cos\ \beta\ \cos\ \alpha - \delta\ + \cos\ \beta\ \cos\ \alpha - \delta} \qquad (21)$$

- Negative $\tau_{42}$

$$\eta_{\tau-} = \frac{\eta_{g1}\eta_{g2} \sin\ \alpha\ \sin\ \beta - \delta}{\eta_{g1}\eta_{g2} \cos\ \delta\ \cos\ \alpha - \beta\ - \cos\ \beta\ \cos\ \alpha - \delta} \qquad (22)$$

Simpler efficiency expressions are obtained by substitution of one design angle as a function of $\tau_{42}$ and of its reciprocal $i_{42} = 1/\tau_{42}$:

- Positive $\tau_{42}$

$$\eta_{\tau+} = \frac{\eta_{g1}\eta_{g2}\tau_{42}}{\eta_{g1}\eta_{g2}\ 2\tau_{42} - 1\ + 1 - \tau_{42}} = \frac{\eta_{g1}\eta_{g2}}{i_{42}\ 1 - \eta_{g1}\eta_{g2}\ + 2\eta_{g1}\eta_{g2} - 1} \qquad (23)$$

- Negative $\tau_{42}$

$$\eta_{\tau-} = \frac{\eta_{g1}\eta_{g2}\tau_{42}}{\tau_{42} + \eta_{g1}\eta_{g2} - 1} = \frac{\eta_{g1}\eta_{g2}}{i_{42}\ \eta_{g1}\eta_{g2} - 1\ + 1} \qquad (24)$$

It is worth remembering that positive values of $\tau_{42}$ are obtained for $\beta - \delta > 0$, so previous relations must be chosen on the basis of the sign of $\beta - \delta$. To obtain a first estimate of gearbox efficiency, single gear pair efficiencies may be estimated through the classical relation (Nelson and Cipra, 2005-b), that provide a rough estimate of basic efficiencies $\eta_{g1}$ and $\eta_{g2}$:

$$1 - \eta_g = \lambda_g = 0.2\left(\frac{1}{z_1} + \frac{1}{z_2}\right) \qquad (25)$$

in which $z_1$ and $z_2$ are the tooth number of the two gears in the gear pair. If more precise information about gear pair efficiencies is available, a more precise result may be obtained from Eqs. (23) and (24).

## 4. INTERNAL KINEMATICS

The model of unbalance forces and torques due to inertial effects is now developed with regard to the embodiment and kinematic schemes presented in Figure 1 and Figure 2, as in this case unbalance effects are more relevant and, moreover, the embodiment leaves more space for engineering solutions.

For the development of the dynamic model in relation to unbalance forces and torques, the system can be simplified by considering only the motion of bodies 2 and 3; the output body 4 is balanced and rotating around a fixed axis, so it does not yield any static or dynamic unbalance effect.

Figure 7 shows the reduced scheme and the used reference systems and notation. To simplify the development of kinematic and dynamic equations, according to the spherical nature of the mechanism, the origins of all used reference systems coincide with the center of the motion **O**; therefore:

a) reference systems are attached to frame 1 and carrier 2; they share the revolute axis (*y* direction); the rotation angle $\vartheta_{12}(t)$ from $x_1$ to $x_2$ completes the information about their relative position

b) a (constant) rotation around $z_2$ of angle $\alpha$ yields to an intermediate reference system named *a*; the nutating body 3 is reached by a rotation around the $y_a = y_3$ axis, i.e. the second revolute joint, with angle $\vartheta_{23}(t)$ from $x_a$ to $x_3$.

By design, the carrier body 2 is symmetric with respect to the $x_2$-$y_2$ plane, therefore in its local reference frame its center of mass $\mathbf{G}_2$ has coordinates $\left[G_{2x}, G_{2y}, 0\right]^T$; similarly, by design, the nutating body has its center of mass $\mathbf{G}_3$ lying on the local $y_3$ axis, with coordinates $\left[0, G_{3y}, 0\right]^T$.

Based on previous considerations and notation, it is possible to express the rotations of the moving bodies and the positions of their centers of mass, along with their time derivatives with respect to the fixed reference frame; according to the study purpose, the system is considered in steady state motion ( $\ddot{\vartheta}_{12} = \dot{\omega}_{12} = 0, \ddot{\vartheta}_{23} = \dot{\omega}_{23} = 0$ ), so we obtain:

1) rotation matrices

$$\mathbf{R}_{12} = \begin{bmatrix} \cos\vartheta_{12} & 0 & \sin\vartheta_{12} \\ 0 & 1 & 0 \\ -\sin\vartheta_{12} & 0 & \cos\vartheta_{12} \end{bmatrix} \qquad (26)$$

$$\mathbf{R}_{13} = \begin{bmatrix} \cos\vartheta_{12}\cos\alpha\cos\vartheta_{23} - \sin\vartheta_{12}\sin\vartheta_{23} & -\cos\vartheta_{12}\sin\alpha \\ \sin\alpha\cos\vartheta_{23} & \cos\alpha \\ -\sin\vartheta_{12}\cos\alpha\cos\vartheta_{23} - \cos\vartheta_{12}\sin\vartheta_{23} & \sin\vartheta_{12}\sin\alpha \\ \cos\vartheta_{12}\cos\alpha\sin\vartheta_{23} + \sin\vartheta_{12}\cos\vartheta_{23} \\ \sin\alpha\sin\vartheta_{23} \\ -\sin\vartheta_{12}\cos\alpha\sin\vartheta_{23} + \cos\vartheta_{12}\cos\vartheta_{23} \end{bmatrix} \qquad (27)$$

2) angular velocities

$${}_1\boldsymbol{\omega}_{12} = \begin{bmatrix} 0 & \dot{\vartheta}_{12} & 0 \end{bmatrix}^T \text{ and } {}_a\boldsymbol{\omega}_{23} = \begin{bmatrix} 0 & \dot{\vartheta}_{23} & 0 \end{bmatrix}^T \qquad (28)$$

and w.r.t. fixed reference frame:

$${}_1\boldsymbol{\omega}_{23} = \begin{bmatrix} -\cos\vartheta_{12}\sin\alpha\,\dot{\vartheta}_{23} & \cos\alpha\,\dot{\vartheta}_{23} & \sin\vartheta_{12}\sin\alpha\,\dot{\vartheta}_{23} \end{bmatrix}^T \qquad (29)$$

$${}_1\boldsymbol{\omega}_{13} = \begin{bmatrix} -\cos\vartheta_{12}\sin\alpha\,\dot{\vartheta}_{23} & \dot{\vartheta}_{12} + \cos\alpha\,\dot{\vartheta}_{23} & \sin\vartheta_{12}\sin\alpha\,\dot{\vartheta}_{23} \end{bmatrix}^T \qquad (30)$$

3) angular accelerations

$${}_1\dot{\boldsymbol{\omega}}_{12} = \begin{matrix} 0 & 0 & 0 \end{matrix}^T \text{ and } {}_1\dot{\boldsymbol{\omega}}_{13} = \sin\alpha \begin{bmatrix} \sin\vartheta_c & 0 & \cos\vartheta_c \end{bmatrix}^T \dot{\vartheta}_{12}\dot{\vartheta}_{23} \qquad (31)$$

4) positions and accelerations of centers of mass w.r.t. fixed reference frame

$$\begin{aligned} {}_1\mathbf{G}_2 &= \begin{bmatrix} \cos\vartheta_{12} & G_{2x} & G_{2y} & -\sin\vartheta_{12} & G_{2x} \end{bmatrix}^T \\ {}_1\ddot{\mathbf{G}}_2 &= \begin{bmatrix} -\cos\vartheta_{12} & 0 & \sin\vartheta_{12} \end{bmatrix}^T G_{2x}\dot{\vartheta}_{12}^2 \end{aligned} \qquad (32)$$

$$\begin{aligned} {}_1\mathbf{G}_3 &= \begin{bmatrix} -\cos\vartheta_{12} & \sin\alpha & \cos\alpha & \sin\vartheta_{12} & \sin\alpha \end{bmatrix}^T G_{3y} \\ {}_1\ddot{\mathbf{G}}_3 &= \sin\alpha \begin{bmatrix} \cos\vartheta_{12} & 0 & -\sin\vartheta_{12} \end{bmatrix}^T G_{3y}\dot{\vartheta}_2^2 \end{aligned} \qquad (33)$$

As a final remark concluding kinematics, we remind that the system has only 1 degree of freedom, and according to equation it is $\dot{\vartheta}_{23} = \omega_{23} = \tau_{32\_2}\dot{\vartheta}_{12} = \tau_{32\_2}\omega_{12}$.

## 5. DYNAMICS

An inverse dynamic model of the system, for given input velocity $\omega_{12}$, is obtained by applying the Newton-Euler equations to the nutating body 3 and then to the carrier body 2, so that the total reaction forces and torques transmitted to the frame due to inertial excitation are determined (Fanghella et al., 2003; Fisette et al., 2002; Callegari et al., 2013).

Such a model is obtained by considering that body 3 is supported by revolute joint with body 2 and is connected to bodies 1 and 4 with gear joints. Each of these joints apply a load to body 3. Nonetheless, the present dynamic analysis is focused on determining the effect of unbalanced inertial forces to the frame of the gearbox, so forces due to the two gear pairs, that are balanced internally to the gearbox, are not taken into account in the dynamic model. In practice, the gearbox is studied in motion conditions, but assuming that the transmitted torque and any loss are null and that, as it is in the real system, all inertial effects of the moving bodies are supported by the bearings constraining body 3 to body 2 and then, in turn, body 2 to body 1. This approach is very common in the study of rotor dynamics, where the dynamic behavior of the system is often considered without taking into account the external loads applied to the system except inertial ones (Genta, 2009, Part III).

In the following equations, all vector entities in such equations are projected to the fixed reference frame, thereby obtaining:

1) nutating body

$$\begin{cases} {}_1\mathbf{F}_{23} = m_3 \ {}_1\ddot{\mathbf{G}}_3 \\ {}_1\mathbf{M}_{23} = {}_1 \ \mathbf{J}_3 \ \dot{\boldsymbol{\omega}}_{13} + {}_1 \ \tilde{\boldsymbol{\omega}}_{13} \ \mathbf{J}_3 \ \boldsymbol{\omega}_{13} \end{cases} \quad (34)$$

in which

- ${}_1\mathbf{F}_{23}$ and ${}_1\mathbf{M}_{23}$ are force and torque transmitted to the carrier body 2 by nutating body 3, due to inertial effects
- ${}_1 \ \mathbf{J}_3$ is the inertial tensor of body 3, expressed in the absolute reference frame through the transformation:

$${}_1 \ \mathbf{J}_3 \ = \ \mathbf{R}_{13} \ {}_3 \ \mathbf{J}_3 \ \mathbf{R}_{13}{}^T \quad (35)$$

Due to the rotational symmetry of the nutating body, its inertia tensor is diagonal, with $J_{3x} = J_{3z}$:

$${}_3 \ \mathbf{J}_3 \ = \begin{bmatrix} J_{3x} & 0 & 0 \\ 0 & J_{3y} & 0 \\ 0 & 0 & J_{3x} \end{bmatrix} \quad (36)$$

carrier body

$$\begin{cases} {}_1\mathbf{F}_{12} = m_2 \ {}_1\ddot{\mathbf{G}}_2 \ - \ -{}_1\mathbf{F}_{23} \\ {}_1\mathbf{M}_{12} = {}_1 \ \tilde{\boldsymbol{\omega}}_{12} \ \mathbf{J}_2 \ \boldsymbol{\omega}_{12} \ - \ -{}_1\mathbf{M}_{23} \end{cases} \quad (37)$$

in simplified form since ${}_f\dot{\boldsymbol{\omega}}_{fc} = 0$, from which reaction forces and torques transmitted to the frame due to inertia forces, i.e. the static and dynamic unbalance of the system, can be finally determined (${}_1\mathbf{F}_{12}$ and ${}_1\mathbf{M}_{12}$). The inertia tensor of carrier 2 w.r.t. fixed frame ${}_1 \ \mathbf{J}_2$ is obtained as previously, starting from its local body inertial tensor, which is, according to its symmetry:

$$ {}_2\mathbf{J}_2 = \begin{bmatrix} J_{2xx} & J_{2xy} & 0 \\ J_{2xy} & J_{2yy} & 0 \\ 0 & 0 & J_{2zz} \end{bmatrix} \tag{38} $$

By substituting all previous relations into the Newton-Euler equations and simplifying, the following results are obtained:

$$ {}_1\mathbf{F}_{23} = m_3 \sin\ \alpha\ G_{3y} \begin{bmatrix} \cos\ \vartheta_{12} \\ 0 \\ -\sin\ \vartheta_{12} \end{bmatrix} \dot{\vartheta}_{12}^2 \tag{39} $$

$$ {}_1\mathbf{M}_{23} = -\sin\ \alpha\ \ \cos\ \alpha\ \ J_{3x} - J_{3y}\ \dot{\vartheta}_{12} - J_{3y}\dot{\vartheta}_{23} \begin{bmatrix} \sin\ \vartheta_{12} \\ 0 \\ \cos\ \vartheta_{12} \end{bmatrix} \dot{\vartheta}_{12} \tag{40} $$

and then, as a complete result:

$$ {}_1\mathbf{F}_{12} = \ m_3 \sin\ \alpha\ G_{3y} - m_2 G_{2x} \begin{bmatrix} \cos\ \vartheta_{12} \\ 0 \\ -\sin\ \vartheta_{12} \end{bmatrix} \dot{\vartheta}_{12}^2 \tag{41} $$

$$ {}_1\mathbf{M}_{12} = \ -\sin\ \alpha\ \ \cos\ \alpha\ \ J_{3x} - J_{3y}\ \dot{\vartheta}_{12} - J_{3y}\dot{\vartheta}_{23}\ - J_{2xy}\dot{\vartheta}_{12} \begin{bmatrix} \sin\ \vartheta_{12} \\ 0 \\ \cos\ \vartheta_{12} \end{bmatrix} \dot{\vartheta}_{12} \tag{42} $$

Obviously, ${}_1\mathbf{F}_{12}$ and ${}_1\mathbf{M}_{12}$ are two orthogonal vectors rotating with the carrier body 2, whose amplitudes depend quadratically on the rotation velocities; moreover, all terms coming out from the nutating body vanish for design angle $\alpha$=0. Due to the gyroscopic effect, the moment ${}_1\mathbf{M}_{12}$ depends on both velocities $\dot{\vartheta}_{12}$ and $\dot{\vartheta}_{23}$, but, reminding that such velocities are related by the transmission ratio $\tau_{32\_2}$, we get the following final expressions for the amplitudes of force and moment over $\dot{\vartheta}_{12}^2$:

$$ S_u = \frac{\left|{}_1\mathbf{F}_{12}\right|}{\dot{\vartheta}_{12}^2} = m_3 \sin\ \alpha\ G_{3y} - m_2 G_{2x} \tag{43} $$

$$D_u = \frac{\left|{}_1\mathbf{M}_{12}\right|}{\dot{\vartheta}_{12}^2} = \sin\ \alpha \quad \tau_{32\_2} J_{3y} - \cos\ \alpha \quad J_{3x} - J_{3y} \quad - J_{2xy} \tag{44}$$

that depend only on the kinematic and inertial parameters of the system.

In order to avoid static and dynamic unbalances, the system must be designed so that such amplitudes are null or sufficiently small to yield, at nominal speed, acceptable values of force and moment. The first relation has a clear and simple physical interpretation: in order to have null static unbalance, the center of mass of the joined carrier and nutating bodies must lie on the fixed axis of rotation of the carrier 2. The second relation is more complex and hard to be physically discussed, as it involves a mix of kinematic, geometrical and inertial parameters. This point will be reconsidered in the numerical example.

## 6. MULTIBODY SIMULATIONS

The analytical results of Section 5 have been validated through dynamic simulations carried out by a commercial multibody software (Creo 2.0 - Mechanism Dynamics), for a geometrical configuration similar to the one of Figure 1, with the following values:

$$\alpha = 10.3° \qquad \tau_{32\_2} = -1.05$$
$$m_2 = 0.04kg \qquad G_{2x} = -3.83mm$$
$$m_3 = 0.1kg \qquad G_{3y} = -8.92mm$$
$$J_{2xy} = -3.08kgmm^2$$
$$J_{3x} = 19.7kgmm^2 \qquad J_{3y} = 20kgmm^2$$

for which, from previous relations, it is: $S_u = 0.00062kgmm$ and $D_u = -0.62kgmm^2$. For an input velocity $\dot{\vartheta}_{12} = 3000rpm$, previous analytical results provide a value of force transmitted to the frame ${}_1F_{12} = 61.2mN$ and of moment ${}_1M_{12} = 61297mNmm$.

The numerical model is defined similarly to previous analytical model, therefore:

- body 2 is connected to frame 1 by a revolute joint (named "pin" joint within Creo), and rotates at the prescribed angular velocity $\dot{\vartheta}_{12}$ thanks to a kinematic servomotor;
- body 3 is connected to body 2 by a revolute joint and rotates, with respect to body 2, at the prescribed angular velocity $\dot{\vartheta}_{23}$ thanks to a kinematic servomotor; the value for $\dot{\vartheta}_{23}$ is chosen according to the value of $\dot{\vartheta}_{12}$ and relation (7)
- no gear pairs are inserted in the model, so bodies 2 and 3 are in motion as in the real system, but no forces/torques are transmitted to the pin joints except inertia ones
- the model has zero degrees of freedom and it is not overconstrained, therefore reaction forces in revolute joints are uniquely defined and can be computed by an inverse dynamic simulation. In particular reaction forces and torques in the joint between links 1 and 2, i.e. ${}_1\mathbf{F}_{12}$ and ${}_1\mathbf{M}_{12}$ , are those considered in the following discussion, as they represent the inertial loads transmitted to the gearbox frame.

Figure 8 shows the *x* component of the static unbalance force ${}_1\mathbf{F}_{12}$ as obtained by the analytical model presented in the previous Sections and by the numerical multibody model. Similarly, Figure 9 shows the *x* component of the dynamic unbalance moment ${}_1\mathbf{M}_{12}$, analytical and numerical. Both figures show a perfect match of the two approaches.

## 7. DISCUSSION ABOUT A BALANCING GEOMETRY

The balancing of the planetary gear train requires that both relations (43) and (44) are null. Some design parameters, namely $\alpha$ and $\tau_{32\_2}$, are related to the functional and gear design of the mechanism and cannot be used to balance it.

Regarding the static balancing, the first term of eq. 43 ($m_3 \sin \alpha \; G_{3y}$) is mostly determined by embodiment requirements of gears 1 and 3 (Figure 1, Figure 4), so the only possibility is to add a counterweight to the carrier body 2, opposite to the position of nutating body center of mass, creating a static moment to equilibrate the nutating body unbalance Figure 10-a shows a possible solution, in which the counterweight is obtained as a lateral expansion of the input shaft (carrier body 2).

Regarding dynamic balancing, the value of $D_u$ (eq. 44) is composed by the sum of three terms: a) $\sin \alpha \; \tau_{32\_3} J_{3y}$, b) $-\sin \alpha \cos \alpha \; J_{3x} - J_{3y}$ and c) $-J_{2xy}$.

As shown by the data in the numerical example, for practical geometries, the term b) is negligible as $J_{3x} \cong J_{3y}$, so balancing may be mainly obtained equating a) and c). Again, term a) depends on the mechanism functional design and on the inertial properties of nutating body; reducing the inertia $J_{2y}$ may help, but there are limitations due to embodiment design of nutating gears. Then the main balancing effect may be conceptually achieved by appending couple of masses to the carrier body 2 to obtain the required $J_{2xy}$ value, as shown schematically in Figure 10-b.

As a matter of fact, the complete, static and dynamic, balancing of a planetary bevel gear train requires a complex geometric design of the real shapes of carrier and nutating bodies that can be hardly carried out manually, as both effects must be dealt with concurrently. Fortunately, available software technologies for parametric manipulation and optimization of 3D solid models allow to search for solutions of the considered problem that are feasible both from the functional and manufacturing points of view. For the considered case study, a possible geometric solution is shown in Figure 10-c: it has been obtained by a feasibility design problem, carried out within Creo, with the distance of the center of mass from the fixed rotation axis and the deviation inertia moment of the assembled system (formed by bodies carrier, bearing, nutating gear and counterweight), as design constraints; dimension of the counterweight body (pink body in Figure 10-c ) are adopted as design parameters. The resulting geometry is both well balanced and feasible from a technological and embodiment points of view.

## 8. CONCLUSIONS

The paper presents the main geometric, functional and dynamic features of a nutating gearbox based on bevel gears. In the first part of the paper, complete explicit expressions of gearbox transmission ratio and efficiency in term of its main design parameters are obtained, for two possible different internal arrangements of the gear pairs.

The second part of the paper is devoted to the development, verification and application of design conditions needed to guarantee the elimination of inertial loads transmitted to the gearbox frame due to the internal motion of bodies. The presented approach is based

on an inverse dynamic model of the gearbox considered as an open chain. In this way, explicit balancing conditions are obtained in term of a very limited number of system geometric and kinematic parameters and body inertial properties. Then obtained results are verified through a numerical multibody simulation, carried out by a commercial CAE software tool.

Finally the balancing conditions are used to define an embodiment design, for the considered case study, allowing manufacturing and functional feasibility, along with complete balancing of the gearbox.

The presented approach does not consider some dynamic effects, such as gear meshing forces and body and joint elasticity. Although they may be relevant in the vibrational and noise characteristics of a gearbox, in the present case, due to the high stiffness of the considered system and to the high frequencies of tooth meshing they do not play a significant role in the considered problem. Nonetheless, future advancements of this research will possibly consider them, to obtain more complete dynamic models and design information.





## REFERENCES

Barbagelata, A., Fanghella, P., Landò, R. (2003). Innovative Drive System for Electric Windows for Cars Based on a Space Born Gearbox (Spacegear). *International Symposium CONVERGENCE '03: Aeronautics, Automotive & Space*, Paris, France

Callegari, M., Fanghella, P., Pellicano, F. (2013). *Mechanics of Machines*. Cittastudi (in Italian)

Day, C., Akeel, H. A., Gutkowsky, L. J. (1983). Kinematic Design and Analysis of Coupled Planetary Bevel-gear Trains. *Transactions of the ASME, Journal of Mechanical Design* 105(3):441–444

Del Pio, G., Pennestrì, E., Valentini, P.P. (2013). Kinematic and Power-flow Analysis of Bevel Gears Planetary Gear Trains with Gyroscopic Complexity. *Mechanism and Machine Theory* 70:523–537

Fanghella, P. (2009). A Computational Approach for the Evaluation of Single d.o.f. Planetary Gear Efficiency. In Kecskeméthy, A., Müller, A. Eds. *Computational kinematics*. Springer, 367-374

Fanghella, P., Galletti, C., Torre, G. (2003). An Explicit Independent-Coordinate Formulation for the Equations of Motion of Flexible Multibody Systems. *Mechanism and Machine Theory* 38(5):417-437

Fisette, P., Postiau, T., Sass, L. and Samin, J. C. (2002). Fully Symbolic Generation of Complex Multibody Models. *Mechanics of structures and machines* 30(1):31–82

Genta, G. (2009). *Vibration Dynamics and Control*. Springer

Landò, R. (2001): Analisys and Design of a Nutating Planetary Gear-train. MS Thesis, University of Genoa, Department of Mechanical Engineering (in Italian)

Ligang, Y., Bing, G., Shujuan, H., Guowu, W., Dai, J. S. (2010). Mathematical Modeling and Simulation of the External and Internal Double Circular-arc Spiral Bevel Gears for the Nutation Drive. *Transactions of the ASME, Journal of Mechanical Design* 132(2): 0210081-02100810

Litvin, F.L., Zheng, Y. (1986). Robotic Bevel-gear Differential Train. *International Journal of Robotics Research* 5(2):75–81

Molyneux, W. G. (1997). The Internal Bevel Gear and its Applications. *Proceedings of the Institution of Mechanical Engineers, Part G: Journal of Aerospace Engineering* 211(1):39-61

Nelson, C. A., Cipra, R. J. (2005-a). Similarity and Equivalence of Nutating Mechanisms to Bevel Epicyclic Gear Trains for Modeling and Analysis. *Transactions of the ASME, Journal of Mechanical Design* 127(2): 269-277

Nelson, C. A., Cipra, R. J. (2005-b). Simplified Kinematic Analysis of Bevel Epicyclic Gear Trains With Application to Power-Flow and Efficiency Analyses. *Transactions of the ASME, Journal of Mechanical Design* 127(2):278–286

Staicu, S. (2008). Inverse Dynamics of a Planetary Gear Train for Robotics. *Mechanism and Machine Theory* 43(7):918–927

Talpasanu, I., Simionescu, P. A. (2012). Kinematic Analysis of Epicyclic Bevel Gear Trains With Matroid Method. *Transactions of the ASME, Journal of Mechanical Design* 134(11):114501-114508

Uyguroglu, M., Demirel, H. (2005). Kinematic Analysis of Bevel-gear Trains Using Graphs. *Acta Mechanica* 177(1):19–27

Yan S., Eiber A. and Schiehlen, W. (2005) Interaction between Electrical and Mechanical Components in Hand-held Electrical Tools. *Mechanics Based Design of Structures and Machines* 33(3):271–292

Zihni B. Saribay, Z. B., Robert C. Bill R. C. (2013). Design analysis of Pericyclic Mechanical Transmission system, *Mechanism and Machine Theory* 61:102–122

Figure 1 bodies and pairs in the considered gear train

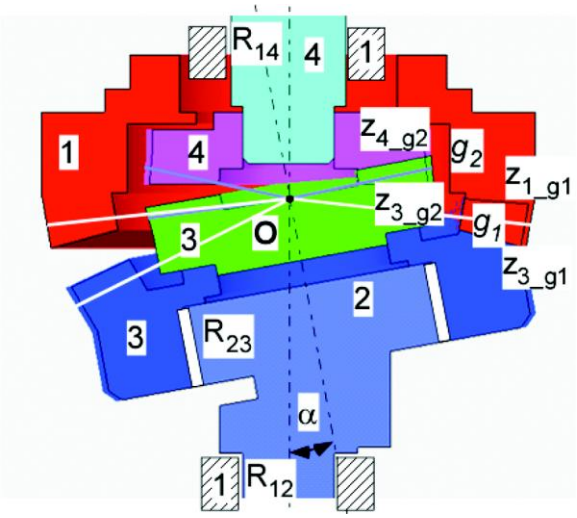

Figure 2 geometric parameters in the considered gear train

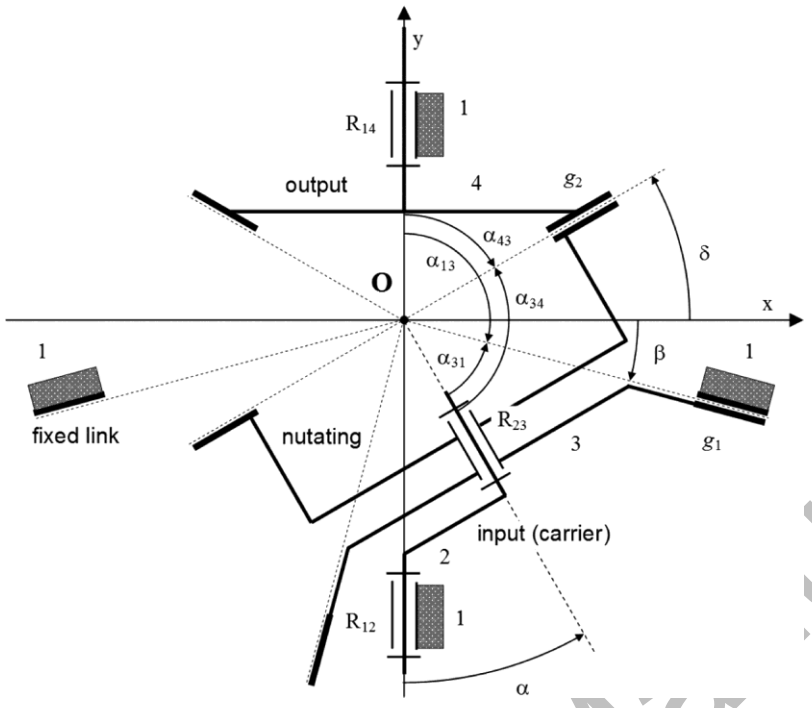

Figure 3 alternative geometric configuration

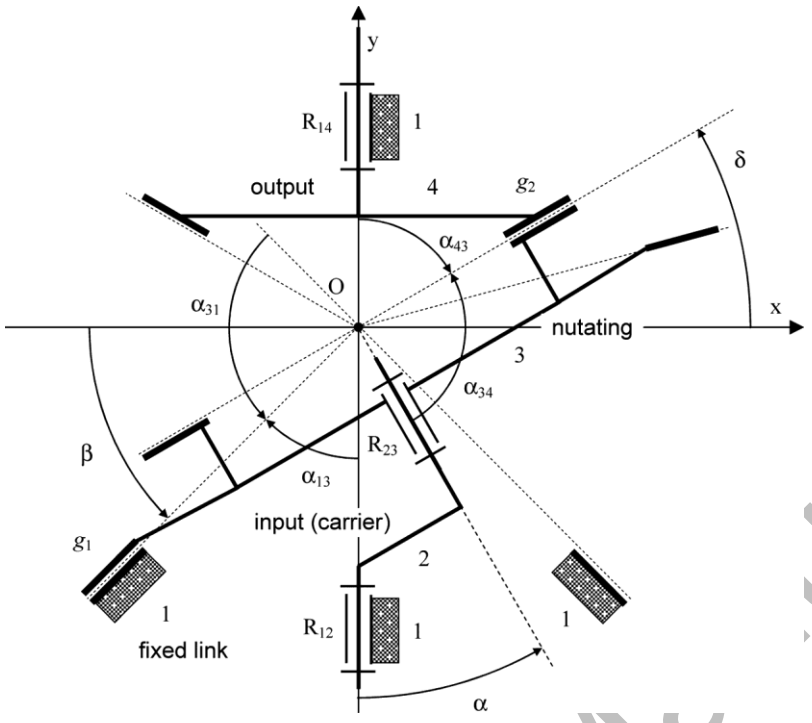

Figure 4 nutating gear geometries

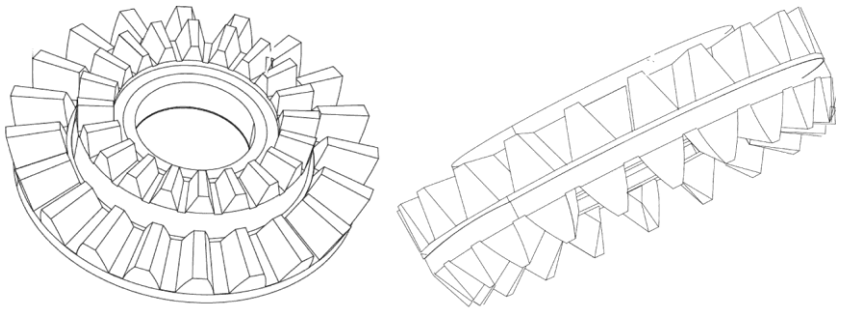

(a) (b)

Figure 5 General bevel gear

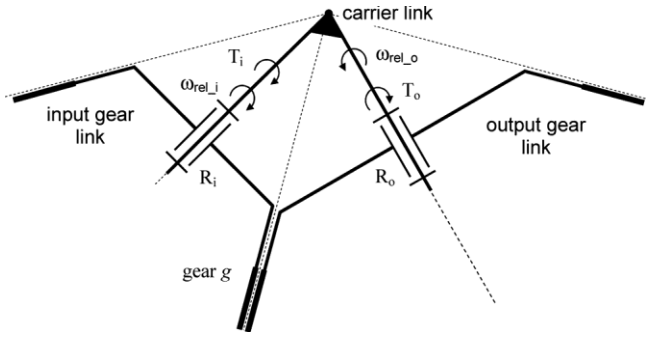

Figure 6 Power flow in gear

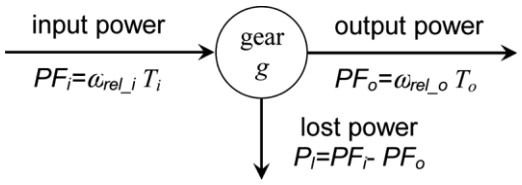

Figure 7 Reference systems and notation for dynamic model

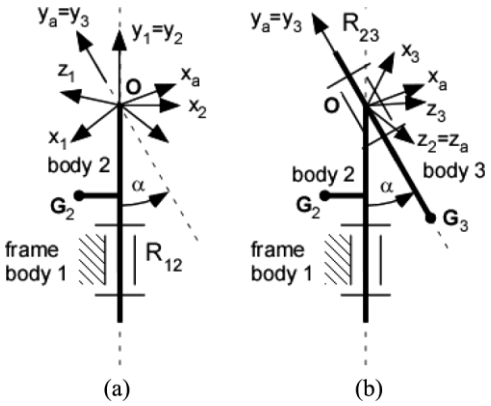

Figure 8 x component of the unbalance force: analytical (left), simulated (right)

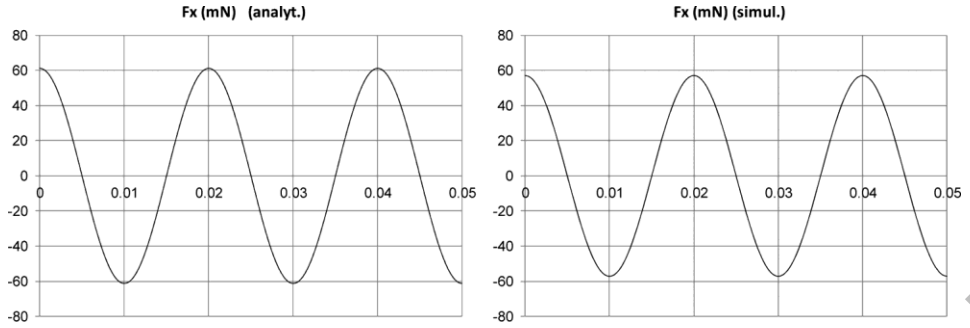

Figure 9 x component of the unbalance moment: analytical (left), simulated (right)

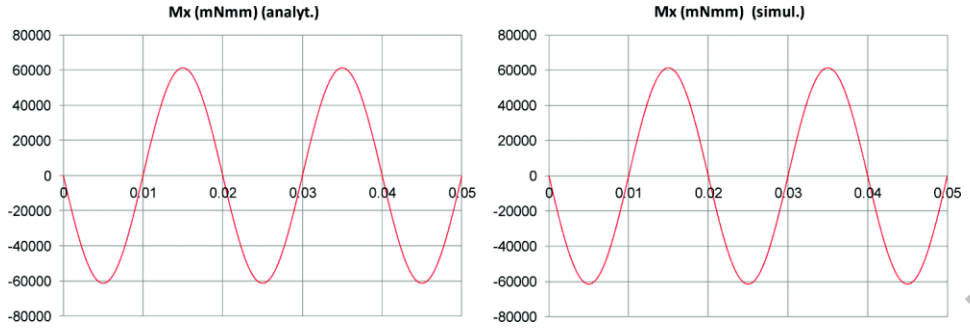

Figure 10 approach to gearbox balancing: a) conceptual static balancing, b) conceptual dynamic balancing, c) actual balanced geometry